

**$g$  factors of coexisting isomeric states in  $^{188}\text{Pb}$** M. Ionescu-Bujor,<sup>1</sup> A. Iordachescu,<sup>1</sup> C. A. Ur,<sup>2</sup> N. Marginean,<sup>1</sup> G. Suliman,<sup>1</sup> D. Bucurescu,<sup>1</sup> F. Brandolini,<sup>2</sup> F. Della Vedova,<sup>3</sup> S. Chmel,<sup>4</sup> S. M. Lenzi,<sup>2</sup> R. Marginean,<sup>1</sup> N. H. Medina,<sup>5</sup> D. R. Napoli,<sup>3</sup> P. Pavan,<sup>2</sup> and R. V. Ribas<sup>5</sup><sup>1</sup>*National Institute for Physics and Nuclear Engineering, Bucharest, Romania*<sup>2</sup>*Dipartimento di Fisica dell' Università and INFN, Sezione di Padova, Padova, Italy*<sup>3</sup>*Laboratori Nazionali di Legnaro, Legnaro, Italy*<sup>4</sup>*Helmholtz-Institut für Strahlen- und Kernphysik, Universität Bonn, D-53115 Bonn, Germany*<sup>5</sup>*Instituto de Física, Universidade de São Paulo, São Paulo, Brazil*

(Received 18 December 2009; published 24 February 2010)

The  $g$  factors of the  $12^+$ ,  $11^-$ , and  $8^-$  isomeric states in  $^{188}\text{Pb}$  were measured using the time-differential perturbed angular distribution method as  $g(12^+) = -0.179(6)$ ,  $g(11^-) = +1.03(3)$ , and  $g(8^-) = -0.037(7)$ . The  $g$  factor of the  $12^+$  state follows the observed slight down-sloping evolution of the  $g$  factors of the  $i_{13/2}^2$  neutron spherical states with decreasing  $N$ . The  $g$  factors of the  $11^-$  and  $8^-$  isomers proposed as oblate and prolate deformed states, respectively, were interpreted within the rotational model, using calculated and empirical  $g$  factor values for the involved single-particle orbitals.

DOI: [10.1103/PhysRevC.81.024323](https://doi.org/10.1103/PhysRevC.81.024323)

PACS number(s): 21.10.Ky, 21.10.Tg, 21.60.Ev, 27.80.+w

**I. INTRODUCTION**

The shape coexistence phenomenon in neutron-deficient Pb isotopes is currently a subject of great interest. As a result of the shell closure at  $Z = 82$ , these nuclei are spherical in the ground state, but the combined effect of the proton shell gap and the large number of valence neutrons outside the closed  $N = 126$  core (in this case, neutron holes) results in an important lowering of the energy of proton particle-hole  $\pi(np-nh)$  excitations [1] which leads to changes in the nuclear shape. The observation of low-lying excited  $0^+$  states is one of the essential experimental fingerprints. Detailed  $\alpha$ -decay and  $\beta^+$ /electron-capture-decay studies have evidenced the systematic presence of such states in all even-even Pb isotopes between  $A = 184$  and  $A = 200$  [2,3]. In the  $^{186}\text{Pb}$  nucleus located at neutron midshell between  $N = 82$  and 126, the first two excited states above the spherical ground state are assigned as  $0^+$  states for which intruder  $\pi(np-nh)$  configurations were inferred [2]. The  $\pi(2p-2h)$  and  $\pi(4p-4h)$  configurations were associated with low-lying oblate and prolate deformation, respectively, appearing close to the spherical ground state in the total energy surface calculations based on a deformed mean field [4]. Evidence for a predominantly spherical shape of the ground state of Pb isotopes near neutron midshell was recently provided by charge radii measurements in  $^{182-190}\text{Pb}$  [5]. Experimentally the yrast bands in  $^{182-188}\text{Pb}$  have been interpreted as being based on prolate shapes [6–9]. Candidates for collective nonyrast bands built on the coexisting oblate minimum were observed in  $^{186}\text{Pb}$  [10] and  $^{188}\text{Pb}$  [11–13]. Recently performed lifetime measurements in  $^{186,188}\text{Pb}$  confirmed the deformed character of the yrast bands [14–16]. To explain the complex experimental findings, several theoretical models were applied, such as phenomenological shape-mixing calculations [12,13], shell model and interacting boson model [17–19], and beyond mean-field approaches [20–23].

In the  $^{188}\text{Pb}$  nucleus situated near the neutron midshell, the presence of three isomeric states at very close excitation

energies was recently interpreted as a manifestation of triple shape coexistence [11–13]. The decay scheme of the isomeric states is shown in Fig. 1. The  $12^+$  isomer at  $E_x = 2710$  keV was associated with the  $i_{13/2}^2$  two-neutron configuration characteristic of *sphericity*. The 2702-keV  $11^-$  state was interpreted as arising from the excitation of two protons into the  $9/2^-$  [505] and  $13/2^+$  [606] Nilsson orbitals, which are near the Fermi surface at *oblate* deformation, while the  $8^-$  isomer at  $E_x = 2577$  keV was associated with the  $9/2^+$  [624]  $\otimes$   $7/2^-$  [514] two-quasineutron *prolate* configuration [11,12]. The  $g$  factors are important quantities for elucidating the structure of the coexisting states, as they are extremely sensitive to the involved configuration. In this article we report the first results of  $g$ -factor measurements for isomeric states in  $^{188}\text{Pb}$ , aiming to provide further evidence concerning the coexisting structures in Pb nuclei far from stability.

**II. EXPERIMENTAL PROCEDURE AND RESULTS**

The  $g$  factors of the isomeric states in  $^{188}\text{Pb}$  were measured by applying the time-differential perturbed angular distribution (TDPAD) method [24]. The states of interest were populated and aligned in the  $^{164}\text{Er}(^{28}\text{Si},4n)^{188}\text{Pb}$  reaction using a 143-MeV  $^{28}\text{Si}$  pulsed beam (2.5-ns pulse width, 6.2- $\mu\text{s}$  repetition period) delivered by the Legnaro XTU-Tandem accelerator. The target consisted of 1 mg/cm<sup>2</sup> metallic Er, enriched in  $^{164}\text{Er}$  to 82.8%, on which a 5mg/cm<sup>2</sup> Pb layer was evaporated to stop recoiling lead nuclei. The projectiles were stopped in a thick Pb backing. The cubic structure of the lead crystalline lattice allowed the preservation of the isomer nuclear alignment. The target was placed between the pole tips of an electromagnet, and an external magnetic field of 18.6(3) kG was applied perpendicular to the beam-detector plane. The magnetic field was measured with a Hall probe. Two independent runs were performed. In the first run the  $\gamma$  rays were detected by two planar Ge detectors and two

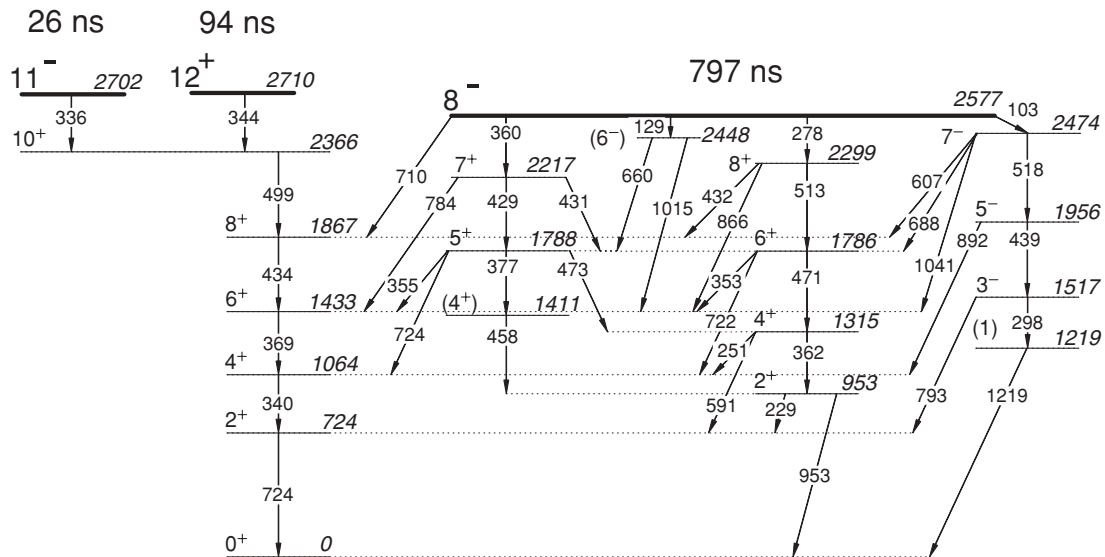


FIG. 1. Decay scheme of the isomeric states in  $^{188}\text{Pb}$  [13]. The assigned half-lives were taken from Ref. [11] ( $11^-$  and  $12^+$  states) and Ref. [26] ( $8^-$  state).

Ge detectors with 20% efficiency each, placed at  $\theta = \pm 135^\circ$  and at  $\theta = \pm 45^\circ$  to the beam direction, respectively. In the second run four large-volume HPGe detectors placed at  $\pm 45^\circ$  and at  $\pm 135^\circ$  with respect to the beam direction were used. In-beam time resolutions of about 7, 10, and 14 ns were obtained for  $\gamma$ -ray energies around 350 keV for planar, medium-volume, and large-volume detectors, respectively.

In the off-line analysis of list-mode data, two-dimensional matrices of energy versus time were formed for each detector. From these matrices time-gated energy spectra and energy-gated time spectra were created. The analysis of  $\gamma$ -ray intensities obtained from energy spectra coincident with the beam pulse (prompt spectra) and with various time intervals between the pulses (delayed spectra) provided information on the isomer population yields and on the branchings at different levels. The isomers were rather weakly populated, the isomer cross section being for each case lower than 10% of the reaction channel cross section. Another difficulty of the experiment was the large contribution of the compound nucleus fission (more than 60% from the total cross section), populating a large number of nuclei, with many isomers and long-lived activities. Substantial contribution from fission was reported recently in a TDPAD pulsed beam experiment using the  $^{168}\text{Er} + ^{28}\text{Si}$  reaction, where several fission nuclei were identified based on the corresponding isomers [25]. Also in the present experiment many isomers with half-lives in the ns to  $\mu\text{s}$  range have been populated in fission nuclei, and the results of this study will be published elsewhere. In the TDPAD experiments the transitions deexciting the isomeric states are usually analyzed for obtaining the Larmor frequency. In the present case, however, because of the very low cross section of the isomeric states and the large background, it was necessary to use a sum of gates on the transitions involved in the decay. To deduce the  $g$  factors of the  $11^-$  and  $12^+$  isomers, the 336-keV  $E1$  and 344-keV  $E2$  deexciting transitions,

respectively, were summed with all  $E2$  transitions below the  $10^+$  state. The deexcitation of the  $8^-$  isomer proceeds via five transitions, with the 360-keV transition taking about half of the intensity [13]. As seen in Fig. 1, the decay is fragmented over many weak paths feeding finally the yrast states. In the data analysis the 360-keV  $E1$  transition and a sum of  $E2$  transitions below the  $8^+$  yrast state were considered. To take into account the opposite sign the angular distribution of dipole and quadrupole transitions, the time spectra  $I(t, \theta, B)$  for the  $E2$  transitions were summed with the time spectra  $I(t, \theta + 90, B)$  for the  $E1$  transitions. Half-lives of 27(5), 99(10), and 820(60) ns were obtained for the  $11^-$ ,  $12^+$ , and  $8^-$  isomers, in accordance with the values reported previously [11,26]. Figure 2 illustrates the background-subtracted time spectrum gated by  $\gamma$  transitions deexciting the low-lying yrast states of  $^{188}\text{Pb}$ , and the least-squares fit which started at 600 ns after the beam pulse, providing the half-life of the  $8^-$  isomeric state.

From the summed time spectra  $N(t, \theta, B)$ , the experimental modulation ratios  $R(t, \theta, B)$  were formed in the standard

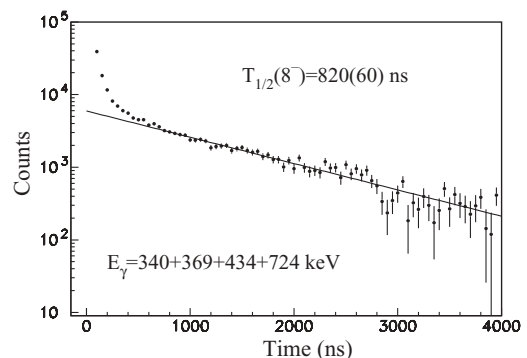


FIG. 2. Time spectrum illustrating the decay of the  $8^-$  isomer in  $^{188}\text{Pb}$ .

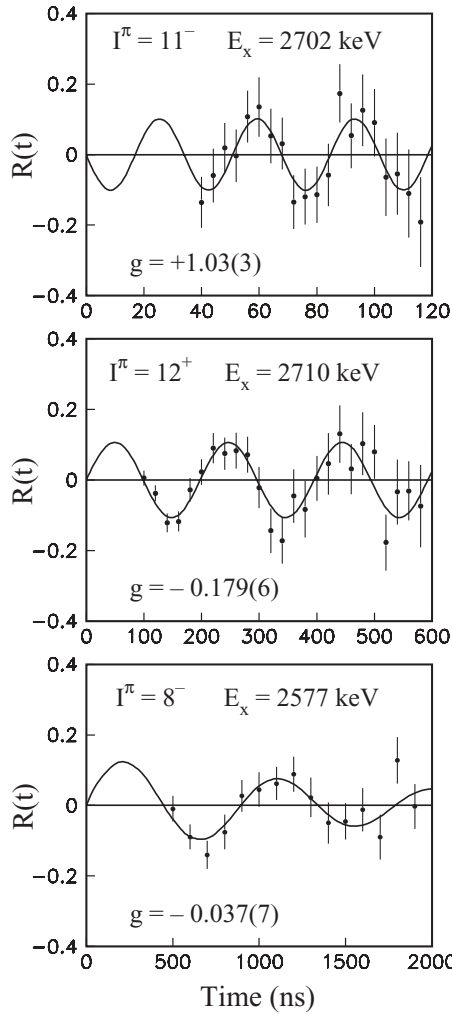


FIG. 3. Experimental modulation ratios for the isomeric states in  $^{188}\text{Pb}$ , in an external magnetic field of 18.6 kG, and the least-squares fits.

way,

$$R_{\text{exp}}(t) = \frac{N(t, \theta, B) - N(t, \theta + 90, B)}{N(t, \theta, B) + N(t, \theta + 90, B)}, \quad (1)$$

and analyzed using the general expression

$$R_{\text{theo}}(t) = b_2 e^{-t/\tau_{\text{rel}}} \cos 2(\theta - \omega_L t), \quad (2)$$

where the  $b_2$  coefficient is related to the angular distribution coefficient  $A_2$  and the alignment degree of the state,  $\tau_{\text{rel}}$  describes the alignment relaxation during the isomer decay, and  $\omega_L$  is the Larmor frequency  $\omega_L = gB\mu_n/\hbar$ . In the case of the  $11^-$  shorter-lived state the modulation ratio obtained using the planar Ge detectors with good time resolution was analyzed. For the  $12^+$  and  $8^-$  isomers, spectra obtained with the medium- and large-volume Ge detectors were used in the analysis. The obtained experimental modulation functions and the corresponding fits are illustrated in Fig. 3. As the yrast transitions used in the analysis have components from all three isomers, in the case of the  $12^+$  and  $8^-$  isomers the analysis of the modulation function could be started at around 100

and 500 ns after the beam burst, respectively. The deduced  $g$ -factor values are  $g(12^+) = -0.179(6)$ ,  $g(11^-) = +1.03(3)$ , and  $g(8^-) = -0.037(7)$ .

The values are corrected for the Knight shift ( $K$ ) and diamagnetic shielding ( $\sigma$ ):  $K(\text{Pb in Pb}) = 1.5(1)\%$  [27] and  $\sigma(\text{Pb}) = -1.0(1)\%$  [28]. No relaxation of the oscillation amplitude was observed on the time scale accessible in the case of the  $11^-$  and  $12^+$  shorter-lived isomers. The longer lifetime of the  $8^-$  isomer allowed to evidence a damping of the oscillation amplitude in spin-rotation spectrum, which most probably is due to the quadrupole interaction with the electric field gradients created by the radiation damage in the cubic lattice of the metallic Pb host. Similar effects have been previously reported in TDPAD studies using the Pb host [29,30].

### III. DISCUSSION

The  $12^+$  isomeric states appear systematically in even Pb isotopes down to  $A = 188$ , and their  $g$  factors were previously determined by applying the TDPAD method in  $^{192-200,206}\text{Pb}$  [31]. The  $g(12^+)$  values are displayed in Fig. 4 together with the presently measured  $g$  factor in  $^{188}\text{Pb}$ . Assuming a pure  $(i_{13/2})^2$  two-neutron configuration for the  $12^+$  state, the additivity rule predicts that  $g(12^+) = g(13/2^+)$ . The  $13/2^+$  states are present in the odd-mass Pb isotopes as long-lived isomers and their  $g$  factors were reported previously for  $^{205}\text{Pb}$  in TDPAD measurements and for  $^{191-197}\text{Pb}$  in collinear laser spectroscopy studies [31]. Very recently the  $g$  factors of the  $13/2^+$  states were determined in the neutron-deficient  $^{183-189}\text{Pb}$ , by applying the in-source resonance ionization spectroscopy technique at the ISOLDE facility [32]. The known  $g$  factors of the  $13/2^+$  states are also illustrated in Fig. 4. We note that the additivity rule holds well for the  $^{205,206}\text{Pb}$  isotopes near the  $N = 126$  shell closure, while for lighter Pb the  $g$  factor of the  $12^+$  states are slightly larger than

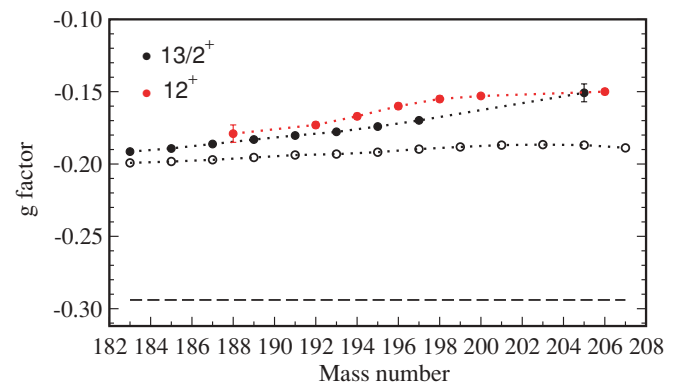


FIG. 4. (Color online) Experimental  $g$  factors for the  $13/2^+$  and  $12^+$  neutron isomers in Pb isotopes (Refs. [31,32] and present work), represented in black solid symbols (middle curve) and red solid symbols (top curve), respectively. The calculated  $g$  factors for the  $13/2^+$  states within the theory of finite Fermi systems [35] are shown by open symbols. The  $g$ -factor values are connected by dotted lines to guide the eye. The Schmidt value for the  $\nu i_{13/2}$  orbital is shown by a dashed line.

$g(13/2^+)$ , indicating small additional contributions. As seen in the Fig. 4, the  $g$  factors of the  $13/2^+$  and  $12^+$  isomers follow a slight down-sloping evolution with decreasing  $N$ , toward the Schmidt line ( $g_{\text{Schm}} = -0.294$ ). This dependence of the  $g$  factors on the neutron number has been attributed to the reduction of the  $M1$  core polarization due to the blocking of  $i_{13/2}-i_{11/2}$  spin flip excitations with decreasing occupation of the  $1i_{13/2}$  shell [33,34]. The observed smooth behavior of the  $g$  factor confirms that the  $i_{13/2}^n$  states in neutron-deficient Pb with  $A \leq 190$  are similar to those in the spherical heavier Pb isotopes.

Detailed magnetic moment calculations in medium-mass and heavy spherical nuclei were very recently performed within the theory of finite Fermi systems [35], taking into account nuclear-medium-modified amplitudes for the exchange of one pion and one  $\rho$  meson. Besides the known orbital and spin terms, a new tensor contribution has been incorporated in the theory. More than 100 magnetic moments of ground and some isomeric states have been calculated and compared to the experimental data. The calculated  $g$  factors for the  $i_{13/2}$  states along the Pb isotopes are shown in Fig. 4. The good description of the experimental data confirms the fact that these states do not lose the spherical shape even very far from the  $\beta$ -stability valley.

While the  $12^+$  isomer has a dominant spherical structure, the  $8^-$  and  $11^-$  isomers were identified as deformed high- $K$  isomers, and band structures based on these states have been established [13]. Calculations within the configuration-constrained potential energy surface framework, performed with the deformed Woods-Saxon potential, gave a prolate deformation of  $\beta_2 = 0.26$  for the  $K^\pi = 8^-$  two-quasineutron isomer in  $^{188}\text{Pb}$  [36] and an oblate deformation of  $\beta_2 = -0.19$  for the  $K^\pi = 11^-$  two-quasiproton isomer in  $^{188}\text{Pb}$  [37]. The measured  $g$  factors for these states provide useful information for the underlined configurations. The  $g$  factor of a state with  $K = \Omega_1 + \Omega_2$  is given by

$$g = g_R + (g_K - g_R) \frac{K}{I + 1}, \quad (3)$$

where  $g_R$  is the collective  $g$  factor and  $g_K$  is given by the coupling formula

$$g_K = \frac{1}{K} (\Omega_1 g_{\Omega_1} + \Omega_2 g_{\Omega_2}). \quad (4)$$

The calculations were performed with a collective  $g$  factor,  $g_R = 0.28(2)$ . The  $g_\Omega$  values were first calculated within the Nilsson approach, using the potential parameters for the  $N = 5$  and 6 shells from Ref. [38]. The value of  $g_\Omega$  is given by

$$g_\Omega = g_l - (g_l - g_s) \frac{\langle S_z \rangle}{\Omega}, \quad (5)$$

where  $\langle S_z \rangle$  is the average intrinsic spin projection. An effective  $g_s$  value of  $0.6g_s^{\text{free}}$  was used for both proton and neutron configurations. In a second estimate, empirical  $g_\Omega$  values were used based on experimental  $g$  factors of states in the neighboring odd-mass nuclei.

Isomeric states with  $I^\pi = 11^-$  were identified in  $^{188-196}\text{Pb}$  and described by coupling the proton  $9/2^-$  [505] and

$13/2^+$  [606] orbitals. Evidence for a moderate deformation associated with the two-proton excitation was provided by quadrupole moment determinations in  $^{192}\text{Pb}$  [25],  $^{194}\text{Pb}$  [25,39], and  $^{196}\text{Pb}$  [40]. Measurements of  $g$  factors were recently performed for these isomers in  $^{194}\text{Pb}$  and  $^{196}\text{Pb}$ , giving values of  $+1.03(2)$  and  $+1.04(5)$ , respectively [41]. The  $g$  factor determined in the present work for  $^{188}\text{Pb}$ ,  $g(11^-) = +1.03(3)$ , coincides with the values determined in the heavier isotopes, pointing to the stability of the deformed two-proton configuration along the light Pb isotopes. The  $g_\Omega$  values for the involved orbitals,  $g_{9/2^-} = +0.947$  and  $g_{13/2^+} = +1.284$ , have been calculated in Ref. [41] using the Nilsson approach at an oblate deformation around  $-0.18$ . With these values, the  $g$  factor of the  $11^-$  state is derived as  $+1.07(3)$ , in fair agreement with the experimental values. An even better agreement is obtained by using empirical  $g_\Omega = g$ , with values of  $+1.246(14)$  [41] and  $+0.913(1)$  ( $^{209}\text{Bi}$  [31]) for the  $13/2^+$  and  $9/2^-$  states, respectively. The  $g$  factor of the  $11^-$  state is calculated as  $+1.04(3)$ , nicely reproducing the experimental values.

The  $8^-$  isomer in  $^{188}\text{Pb}$  at  $E_x = 2577$  keV was described by coupling the neutron  $9/2^+$  [624] and  $7/2^-$  [514] orbitals. In the Nilsson calculations, the quadrupole deformation was taken as  $\epsilon_2 = +0.25$ , corresponding to the value  $\beta_2 = +0.26$  derived by configuration-constrained potential energy surface using a Wood-Saxon potential [36]. The obtained values of  $\langle S_z \rangle / \Omega$  are  $+0.089$  and  $-0.1$  for the  $9/2^+$  [624] and  $7/2^-$  [514] neutron orbitals, respectively. With these values, the derived  $g_\Omega$  were  $g_{9/2^+} = -0.204$  and  $g_{7/2^-} = +0.230$ , leading to a value of  $+0.019(27)$  for the  $g$  factor of the  $8^-$  state. The error arises from the error of the collective  $g_R$ . In the empirical estimation,  $g_\Omega$  values were obtained from experimental  $g$  factors of low-lying deformed neutron states in neighboring nuclei, namely, the  $7/2^-$  state in  $^{183}\text{Pt}$  ( $N = 105$ ) and the  $9/2^+$  state in  $^{183}\text{Os}$  and  $^{185}\text{Pt}$  ( $N = 107$ ) [31]. The deduced empirical values were  $g_\Omega = +0.207(33)$  for the  $7/2^-$  [514] orbital and  $g_\Omega = -0.268(21)$  for the  $9/2^+$  [624] orbital. With these values, one obtains  $g(8^-) = -0.022(17)$ , which agrees within errors with the experimental value. It is worthwhile to mention that the  $8^-$  isomer described by the  $9/2^+$  [624]  $\otimes$   $7/2^-$  [514] two-quasineutron prolate configuration appears systematically in the  $N = 106$  isotones from the well-deformed neutron-rich  $^{174}\text{Er}$  to the neutron-deficient  $^{188}\text{Pb}$  [42,43]. The presently measured  $g$  factor provides for the first time direct evidence for the two-neutron assigned configuration.

#### IV. CONCLUSIONS

The  $g$  factors of the  $12^+$ ,  $11^-$ , and  $8^-$  isomeric states in the very-neutron-deficient  $^{188}\text{Pb}$  nucleus have been measured by the TDPAD method. The  $g$  factor of the  $12^+$  state follows the observed slight down-sloping evolution of the  $g$  factors of the  $i_{13/2}^2$  neutron spherical states with decreasing  $N$ . The observed smooth behavior of the  $g$  factor confirms that the  $i_{13/2}$  states in very-neutron-deficient Pb preserves the spherical shape assigned in heavier Pb isotopes. The  $g$  factors of the  $11^-$  and  $8^-$  states were satisfactorily interpreted within the rotational model, using calculated and empirical  $g$  factor

values for the involved single-particle orbitals. The  $g$  factor of the  $11^-$  isomeric state with the  $9/2^- [505] \otimes 13/2^+ [606]$  two-proton configuration was found to be remarkably similar to the  $g$  factors in the heavier  $^{194,196}\text{Pb}$  isotopes, pointing to the stability of this moderate oblate two-proton configuration. For the  $8^-$  isomer a very small  $g$  factor has been determined, in accordance with the theoretical estimates for the  $9/2^+ [624] \otimes 7/2^- [514]$  two-quasineutron prolate configuration. The obtained data provide therefore new support concerning the triple shape coexistence in light Pb isotopes near the neutron midshell.

## ACKNOWLEDGMENTS

The authors thank the staff of the LNL XTU-Tandem for the high quality of the delivered pulsed beam and Massimo Loriggiola for preparing the target. Support through the European Community FP6—Integrated Infrastructure Initiative—EURONS Contract No, RII3-CT-2004-506065 is acknowledged. This work was supported by the Romanian National Authority for Scientific Research, Contract IDEI No. 52/2007. N.H.M. and R.V.R. acknowledge financial support from the Brazilian Agency CNPq and the Italian INFN.

- 
- [1] J. L. Wood, K. Heyde, W. Nazarevich, M. Huyse, and P. Van Duppen, *Phys. Rep.* **215**, 101 (1992).
- [2] A. N. Andreyev *et al.*, *Nature (London)* **405**, 430 (2000).
- [3] R. Julin, K. Helariutta, and M. Muikku, *J. Phys. G* **27**, R109 (2001).
- [4] W. Nazarewicz, *Phys. Lett.* **B305**, 195 (1993).
- [5] H. De Witte *et al.*, *Phys. Rev. Lett.* **98**, 112502 (2007).
- [6] D. G. Jenkins *et al.*, *Phys. Rev. C* **62**, 021302(R) (2000).
- [7] J. F. C. Cocks *et al.*, *Eur. Phys. J. A* **3**, 17 (1998).
- [8] A. M. Baxter *et al.*, *Phys. Rev. C* **48**, R2140 (1993).
- [9] J. Heese, K. H. Maier, H. Grawe, J. Grebosz, H. Kluge, W. Meczynski, M. Schramm, R. Schubart, K. Spohr, and J. Styczen, *Phys. Lett.* **B302**, 390 (1993).
- [10] J. Pakarinen *et al.*, *Phys. Rev. C* **75**, 014302 (2007).
- [11] G. D. Dracoulis, A. P. Byrne, A. M. Baxter, P. M. Davidson, T. Kibédi, T. R. McGoram, R. A. Bark, and S. M. Mullins, *Phys. Rev. C* **60**, 014303 (1999).
- [12] G. D. Dracoulis, G. J. Lane, A. P. Byrne, A. M. Baxter, T. Kibédi, A. O. Macchiavelli, P. Fallon, and R. M. Clark, *Phys. Rev. C* **67**, 051301(R) (2003).
- [13] G. D. Dracoulis, G. J. Lane, A. P. Byrne, T. Kibédi, A. M. Baxter, A. O. Macchiavelli, P. Fallon, and R. M. Clark, *Phys. Rev. C* **69**, 054318 (2004).
- [14] A. Dewald *et al.*, *Phys. Rev. C* **68**, 034314 (2003).
- [15] T. Grahn *et al.*, *Phys. Rev. Lett.* **97**, 062501 (2006).
- [16] T. Grahn *et al.*, *Nucl. Phys.* **A801**, 83 (2008).
- [17] A. Frank, P. Van Isacker, and C. E. Vargas, *Phys. Rev. C* **69**, 034323 (2004).
- [18] V. Hellemans, R. Fossion, S. D. Baerdemacker, and K. Heyde, *Phys. Rev. C* **71**, 034308 (2005).
- [19] V. Hellemans, S. De Baerdemacker, and K. Heyde, *Phys. Rev. C* **77**, 064324 (2008).
- [20] R. R. Rodriguez-Guzman, J. L. Egido, and L. M. Robledo, *Phys. Rev. C* **69**, 054319 (2004).
- [21] M. Bender, P. Bonche, T. Duguet, and P.-H. Heenen, *Phys. Rev. C* **69**, 064303 (2004).
- [22] J. L. Egido, L. M. Robledo, and R. R. Rodriguez-Guzman, *Phys. Rev. Lett.* **93**, 082502 (2004).
- [23] M. Bender, G. F. Bertsch, and P.-H. Heenen, *Phys. Rev. C* **73**, 034322 (2006).
- [24] E. Recknagel, in *Nuclear Spectroscopy and Reactions*, edited by J. Cerny (Academic Press, New York, 1974), Part C, p. 93.
- [25] M. Ionescu-Bujor *et al.*, *Phys. Lett.* **B650**, 141 (2007).
- [26] A. P. Byrne *et al.*, *Eur. Phys. J. A* **7**, 41 (2000).
- [27] J. M. Rocard, M. Bloom, and L. B. Robinson, *Can. J. Phys.* **37**, 522 (1959).
- [28] F. D. Feiok and W. R. Johnson, *Phys. Rev. Lett.* **21**, 785 (1968).
- [29] E. Dafni, M. H. Rafailovich, W. A. Little, and G. D. Sprouse, *Phys. Rev. C* **23**, 90 (1981).
- [30] M. Ionescu-Bujor *et al.*, *Phys. Lett.* **B495**, 289 (2000).
- [31] N. J. Stone, *At. Data Nucl. Data Tables* **90**, 75 (2005).
- [32] M. D. Seliverstov *et al.*, *Eur. Phys. J. A* **41**, 315 (2009).
- [33] C. Stenzel, H. Grawe, H. Haas, H.-E. Mahnke, and K. H. Maier, *Nucl. Phys.* **A411**, 248 (1983).
- [34] C. Stenzel, H. Grawe, H. Haas, H.-E. Mahnke, and K. H. Maier, *Z. Phys. A* **322**, 83 (1985).
- [35] I. N. Borzov, E. E. Saperstein, and S. V. Tolokonnikov, *Phys. At. Nucl.* **71**, 469 (2008) [*Yad. Fiz.* **71**, 493 (2008)].
- [36] F. R. Xu, P. M. Walker, and R. Wyss, *Phys. Rev. C* **59**, 731 (1999).
- [37] X. Fu-Rong, *Chin. Phys. Lett.* **18**, 750 (2001).
- [38] T. Bengtsson and I. Ragnarsson, *Nucl. Phys.* **A436**, 14 (1985).
- [39] K. Vyvey, D. Borremans, N. Coulier, R. Coussement, G. Georgiev, S. Teughels, G. Neyens, H. Hübel, and D. L. Balabanski, *Phys. Rev. C* **65**, 024320 (2002).
- [40] K. Vyvey *et al.*, *Phys. Rev. Lett.* **88**, 102502 (2002).
- [41] K. Vyvey, G. D. Dracoulis, A. N. Wilson, P. M. Davidson, A. E. Stuchbery, G. J. Lane, A. P. Byrne, and T. Kibédi, *Phys. Rev. C* **69**, 064318 (2004).
- [42] G. D. Dracoulis *et al.*, *Phys. Lett.* **B635**, 200 (2006).
- [43] G. D. Dracoulis *et al.*, *Phys. Rev. C* **79**, 061303(R) (2009).